DOI: 10.13009/EUCASS2023-519
Aerospace Europe Conference 2023 – 10TH EUCASS – 9TH CEAS

Augmented Pursuit Guidance for Flight Trajectory Shaping

Min-Jea TAHK†, Jong-Chan PARK*, Boseok KIM*, Heekun ROH*, Chang-Hun LEE**
** Department of Aerospace Engineering, KAIST*
291 Daehakro Yuseong, Daejeon, Korea
mjtahk@kaist.ac.kr, champ10060@kaist.ac.kr, kbobo6@kaist.ac.kr,
heekunroh@kaist.ac.kr, lckdgns@kaist.ac.kr

Abstract
This paper proposes a novel approach for trajectory shaping based on pursuit guidance. The relationship between the trajectory shape and the lead angle is derived for a class of trajectories expressed as polynomials of the downrange. Then pursuit guidance is augmented to control the lead angle by treating the lead-angle command as a bias signal in the lead-angle feedback loop. Approximations of the lead-angle command are also suggested for simple implementation and the lead-angle tracking error and the miss distance are analysed for quadratic trajectory. Numerical examples are provided to show that the proposed method is useful for finding a suboptimal trajectory for terminal speed maximization.

1. Introduction

For long-range atmospheric flight vehicles such as long-range missiles and re-entry vehicles, trajectory shaping is essential to optimize the guidance performance specified for the mission. Various feedback guidance laws based on constant-speed and constant-altitude assumptions do not perform satisfactorily for long-range flights with significant speed and altitude changes. Although using the optimal guidance command history approximated by polynomials or neural networks is a practical option, it takes a lot of development time to account for various flight conditions. Real-time computational guidance based on convex programming, which has been extensively studied recently, has a high potential of practical application. Since most convexification procedures for non-convex trajectory optimization problems require linearization of the equations of motion, reliable trajectory initialization is essential for guaranteed convergence of convex programming approaches.

Pursuit Guidance (PG) is a simple guidance law that steers the vehicle's velocity vector to the line-of-sight direction of the target. PG relies on the idea that the target can be intercepted if the lead angle (the angle between the velocity vector and the line of sight to the target) is reduced to zero. Although PG is not effective for precise homing guidance against moving targets [1], it is useful for long-range midcourse guidance since it can efficiently generate a feasible trajectory reaching a stationary target or a pseudo-stationary target such as predicted impact point (PIP). Furthermore, PG can be augmented by adding a time-varying lead-angle bias to control the lead angle and, consequently, to modify the trajectory shape. For convenience, PG with a time-varying lead-angle bias, which has the role of the lead-angle command, is referred to as Augmented Pursuit Guidance (APG) in this paper.

APG proposed in this paper has two features: 1) the lead-angle command is explicitly calculated from the desired trajectory (referred to as 'reference trajectory' here), and 2) the lead angle is controlled by applying APG to track the lead-angle command. Explicit relationship between the reference trajectory's shape and the lead-angle command is derived in this paper. It is found that the lead-angle command can be approximated as an (n-1)-th order polynomial if the reference trajectory is an n-th order polynomial. The history of the zero-effort miss (ZEM) is analysed to confirm that it does not diverge as the missile approaches the target. It is also found that the lead-angle tracking error remains constant after the initial transient phase although it diverges at the last moment.

The proposed method can be applied to various problems related to missile guidance. In this work, we are interested in real-time midcourse guidance for long-range missiles. For example, the optimal lead-angle history of a long-range air-to-air missile for the maximum terminal speed is approximated by a linear function of the range to go, which reduces to zero at the terminal time. This observation implies that a suboptimal trajectory can be easily generated by using a linear lead-angle command. Since the initial value of the bias function is the only parameter to be determined, efficient trajectory initialization for more sophisticated trajectory optimization can be done quickly. Or the proposed method can be directly used for real-time midcourse guidance when a suboptimal trajectory is acceptable. More complex trajectories than a simple quadratic-type trajectory are required if the terminal flight path angle or the flight altitude is constrained. These cases can also be handled well since the shape of a suitable polynomial trajectory is easily found from the optimal trajectory computed off-line.

This paper describes the trajectory shaping based on lead-angle control and provides several examples in Section 2. The characteristics of APG such as lead-angle tracking error and zero-effort miss are then analysed in Section 3.

DOI: 10.13009/EUCASS2023-519

Trajectory optimization for maximization of the terminal speed is treated as numerical experiments in Section 4 and a brief conclusion follows.

2. Trajectory Shaping by Lead-Angle Control

Let x and h denote the downrange and altitude of the missile normalized by the initial range of the predicted intercept point (PIP), X_P;

$$x = X / X_T, \qquad h = H / X_T \tag{1}$$

The line-of-sight (LOS) angle of PIP from the missile, denoted as σ, is defined as

$$\tan\sigma = \frac{h_T - h}{1 - x} \tag{2}$$

where $h_T = H_T / X_T$. The flight path angle of the missile, denoted as γ, is defined as

$$\tan\gamma = \frac{dh}{dx} \tag{3}$$

Then, the lead angle, denoted as λ, is defined as the difference between the flight path angle and the LOS angle:

$$\lambda = \gamma - \sigma \tag{4}$$

Using the trigonometric identity $\tan(a+b) = (\tan a + \tan b)/(1 - \tan a \tan b)$, we see that

$$\tan\lambda = \tan(\gamma - \sigma) = (\tan\gamma - \tan\sigma)/(1 + \tan\gamma\tan\sigma) \tag{5}$$

Then, from (2), (3), and (5), we can express the lead angle as

$$\tan\lambda = \left(\frac{dh}{dx} - \frac{h_T - h}{1 - x}\right) \Big/ \left(1 + \frac{dh}{dx}\frac{h_T - h}{1 - x}\right) \tag{6}$$

Suppose that the reference trajectory h is given as a function of x. Then the lead angle λ can be calculated from (6). This observation implies that an arbitrary trajectory of the missile can be realized if the lead angle of the missile can be controlled to satisfy (6).

Let ξ be the normalized range to go; $\xi \triangleq 1 - x$. Then (6) can be rewritten as

$$\tan\lambda = -\left(\frac{dh}{d\xi} + \frac{h_T - h}{\xi}\right) \Big/ \left(1 - \frac{dh}{d\xi}\frac{h_T - h}{\xi}\right) \tag{7}$$

Suppose that h is expressed as a polynomial of ξ; $h(\xi) = a_0 + a_1\,\xi + a_2\,\xi^2 + \cdots + a_n\xi^n$. We see that $a_0 = h_T$ since $h(0) = h_T$ is required to reach the PIP at the terminal time. Then, $\tan\sigma$ of (3) is rewritten as

$$\tan\sigma = \frac{h_T - h}{\xi} = -(a_1 + a_2\,\xi + \cdots + a_n\xi^{n-1}) \tag{8}$$

We also note that

$$\tan\gamma = \frac{dh}{dx} = a_1 + 2\,a_2\,\xi + \cdots + n\,a_n\xi^{n-1} \tag{9}$$

DOI: 10.13009/EUCASS2023-519

Substituting (8) and (9) into (7), we obtain that

$$\tan\lambda = -\left[a_2\xi + 2a_3\xi^2 + \cdots + (n-1)\,a_n\xi^{n-1}\right] / \left[1 + (a_1 + 2\,a_2\xi + \cdots + n\,a_n\xi^{n-1})(a_1 + a_2\xi + \cdots + a_n\xi^{n-1})\right] \tag{10}$$

It is observed that a polynomial trajectory $h(\xi) = a_0 + a_1\,\xi + a_2\,\xi^2 + \cdots + a_n\xi^n$ can be achieved if the lead angle λ is controlled to satisfy (10).

We now investigate if (10) can be simplified even for large lead angles. The following three approximation methods are compared with the exact implementation for several examples:

(a) Approximation 1 : Simplify the denominator of (10) as 1;

$$\lambda = -\tan^{-1}\left[a_2\xi + 2a_3\xi^2 + \cdots + (n-1)\,a_n\xi^{n-1}\right]$$

(b) Approximation 2 : Replace $\tan\lambda$ by λ;

$$\lambda = -\left[a_2\xi + 2a_3\xi^2 + \cdots + (n-1)\,a_n\xi^{n-1}\right] / \left[1 + (a_1 + 2\,a_2\xi + \cdots + n\,a_n\xi^{n-1})(a_1 + a_2\xi + \cdots + a_n\xi^{n-1})\right]$$

(c) Approximation 3 : Apply both of Approximations 2 and 3;

$$\lambda = -\left[a_2\xi + 2a_3\xi^2 + \cdots + (n-1)\,a_n\xi^{n-1}\right]$$

Example 1: Quadratic Trajectory

Let the reference trajectory be givens as $h(\xi) = h_T + a_1\,\xi + a_2\,\xi^2$. Equation (10) gives the expression of λ as

$$\tan\lambda = -a_2\xi / \left[1 + (a_1 + 2\,a_2\xi)(a_1 + a_2\xi)\right] \tag{11}$$

Given the initial altitude h_0, a_1 and a_2 should satisfy $h_0 = h_T + a_1 + a_2$. Hence, we need one more condition to determine a_1 or a_2. We may specify the peak altitude h_P, which is achieved at $\xi_p = -(1/2)(a_1/a_2)$ as

$$h_P = h_T - (1/4)\,(h_0 - h_T - a_2)^2 / a_2 \tag{12}$$

Or we may specify the initial lead angle, treating it as a design parameter for trajectory shaping. For Approximation 3, λ becomes a simple linear function of ξ;

$$\lambda = -a_2\,\xi. \tag{13}$$

which implies that $\lambda_0 = -a_2$ for Approximation 3.

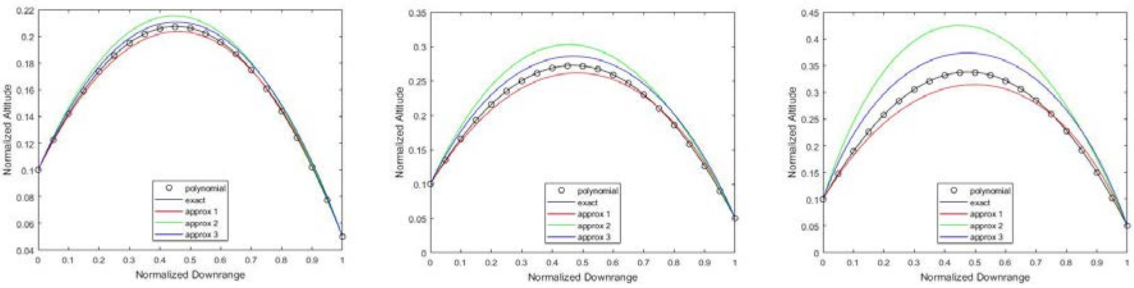

(a) $\lambda_0 = 30\,\text{deg}$ (b) $\lambda_0 = 45\,\text{deg}$ (c) $\lambda_0 = 60\,\text{deg}$

Figure 1: Quadratic Trajectories Produced by Three Approximations (Example 1)

DOI: 10.13009/EUCASS2023-519

Figure 1 compares the trajectories produced by the three approximation methods for three different values of λ_0. In this example, $h_0 = 0.1$ and $h_T = 0.05$. While the exact lead-angle command precisely produces the reference trajectory, Approximations 1 and 3 also generate trajectories close to the reference trajectory. It looks like that the average of the lead angles computed by these two approximations would produce a trajectory a lot closer to the reference trajectory.

Example 2: Cubic Trajectory

In this example, we consider a cubic trajectory $h(\xi) = h_T + a_1\,\xi + a_2\,\xi^2 + a_3\xi^3$ with a constraint on the terminal flight path angle specified as $[dh/d\xi]_{\xi=0} = 0$. Since $a_1 = 0$, λ is expressed as

$$\tan\lambda = -(a_2\xi + 2a_3\xi^2)/\left[1 + (2a_2\xi + 3a_3\xi^2)(a_2\xi + a_3\xi^2)\right] \tag{14}$$

For Approximation 3, the lead angle λ is expressed as

$$\lambda = -(a_2\,\xi + 2a_3\,\xi^2). \tag{15}$$

From $h_0 = h(1) = h_T + a_2 + a_3$ and $\lambda_0 = -a_2 - 2a_3$, we find a_2 and a_3 as $a_2 = 2(h_0 - h_T) + \lambda_0$ and $a_3 = -(h_0 - h_T) - \lambda_0$. We also observe from $dh/d\xi = 2a_2\xi + 3a_3\xi^2$ that the peak altitude occurs at $\xi_P = -(2/3)(a_2/a_3)$ to be

$$h_P = h_T - (4/27)\,(h_0 - h_T - a_3)^3/a_3^2 \tag{16}$$

Figure 2 compares the cubic trajectories produced by the three approximation methods with the exact reference trajectory. Again, we observe that Approximation 1 is the best and Approximation 3 comes next. If (14) is used without approximation, the reference trajectory is precisely generated.

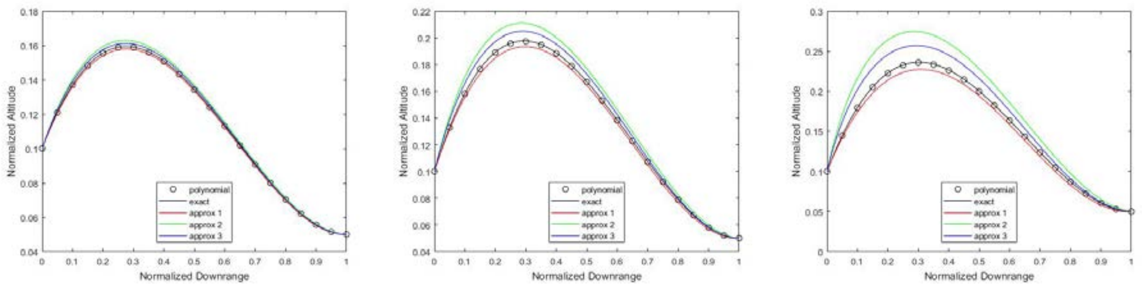

(a) $\lambda_0 = 30\,\text{deg}$ (b) $\lambda_0 = 45\,\text{deg}$ (c) $\lambda_0 = 60\,\text{deg}$

Figure 2: Cubic Trajectories Produced by Three Approximations (Example 2)

Example 3: Fourth-Order Trajectory

Consider a 4th-order trajectory of ξ satisfying $h(0) = h_T$, $h(\xi_1) = h_1$, $h(\xi_2) = h_2$, and $h(1) = h_0$. If Approximation 3 is employed, the coefficients of $h(\xi) = h_T + a_1\,\xi + a_2\,\xi^2 + a_3\xi^3 + a_4\xi^4$ and $\lambda = -(a_2\,\xi + 2a_3\,\xi^2 + 3a_4\,\xi^3)$ can be determined for given λ_0 by solving the following equation:

$$\begin{bmatrix} 1 & 1 & 1 & 1 \\ \xi_1 & \xi_1^2 & \xi_1^3 & \xi_1^4 \\ \xi_2 & \xi_2^2 & \xi_2^3 & \xi_2^4 \\ 0 & -1 & -2 & -3 \end{bmatrix} \begin{bmatrix} a_1 \\ a_2 \\ a_3 \\ a_4 \end{bmatrix} = \begin{bmatrix} h_0 - h_T \\ h_1 - h_T \\ h_2 - h_T \\ \lambda_0 \end{bmatrix} \tag{17}$$

DOI: 10.13009/EUCASS2023-519

Let $\xi_1 = 0.4$, $\xi_2 = 0.6$, and $h_1 = h_2 = 0.2$. Figure 3 shows the 4-th order trajectories produced by the three approximation methods for various λ_0's. We observe that fourth order trajectories are useful if the peak altitude needs to be constrained. For example, flying higher than 20 km altitude may not be desirable if the PIP is subject to a sudden change due to unexpected target motions. The maneuver capability of the missile is severly constrained at high altitudes where the air density is very low.

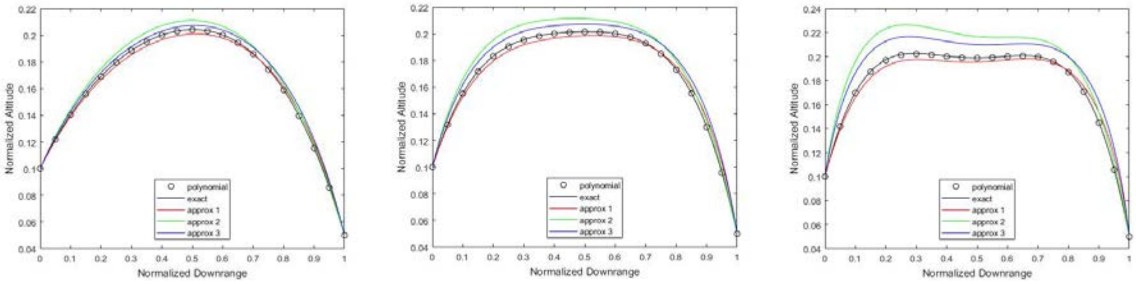

(a) $\lambda_0 = 30$ deg (b) $\lambda_0 = 45$ deg (c) $\lambda_0 = 60$ deg

Figure 3: Fourth-Order Trajectories Produced by Three Approximations (Example 3)

3. Augmented Pursuit Guidance for Lead-Angle Control

In this work, we augment pursuit guidance to control the lead angle. The classical pursuit guidance is modified as

$$a_{com} = N\, V_m (\lambda_{com} - \lambda) \tag{18}$$

where a_{com} is the commanded maneuver acceleration produced perpendicular to the velocity vector, λ_{com} is the commanded lead angle, V_m is the missile speed, and N is the guidance gain. For convenience, the guidance law expressed as (18) is referred to as Augmented Pursuit Guidance (APG) in this paper. Note that APG is a biased pursuit guidance for which $N\, V_m\, \lambda_{com}$ is the bias. In this section, the expressions of the miss distance and the lead-angle tracking error are derived for APG as follows:

Miss Distance

Define $Z = R\, \lambda$ where R is the range from the missile to the target. If λ is small, Z corresponds to the zero effort miss. Now we consider the behaviour of $Z(t)$ during the engagement. Under the assumption that the autopilot has no time lag, the acceleration of the missile, denoted as a, is the sum a_{com} and the acceleration error Δa produced by aerodynamics and the gravity. Then, we have

$$\dot{\gamma} = a / V_m = NV_m (\lambda_{com} - \lambda) / V_m + \Delta a / V_m = N(\lambda_{com} - \lambda) + \Delta a / V_m \tag{19}$$

And the line-of-sight rate $\dot{\sigma}$ is calculated as

$$\dot{\sigma} = -V_m \sin\lambda / R \tag{20}$$

Then, we see that

$$\dot{Z} = \dot{R}\,\lambda + R\,\dot{\lambda} = -V_c \lambda + R(\dot{\gamma} - \dot{\sigma}) = -V_m \cos\lambda\, \lambda + NR(\lambda_{com} - \lambda) + V_m \sin\lambda + (R / V_m)\Delta a \tag{21}$$

Equation (21) is further simplified by the assumption that λ is small;

$$\dot{Z} = -N\, Z + b + (R / V_m)\Delta a \tag{22}$$

DOI: 10.13009/EUCASS2023-519

where $b = N\,R\,\lambda_{com}$. Since the dynamics of Z is stable, the time history of Z is bounded if b and Δa are bounded. However, Z does not converge to zero, in general.

Changing the independent variable of (22) from t to $x = X / X_f$ and assuming γ small, we obtain

$$dZ / dx = kR(\lambda_{com} - \lambda) + (RX_f / V_m^2)\,\Delta a = -k\,Z + B \tag{23}$$

where $k = NX_f / V_m$, $\tau = X_f / V_m^2$, and $B = k\,R\,\lambda_{com} + \tau R\,\Delta a$. The range can be approximated as $R = R_0(1-x)$. If λ_{com} is chosen as $\lambda_{com} = b_0(1-x)$ and Δa is constant, then B becomes a 2nd-order polynomial of x, written as

$$B = k\,R_0\,b_0\,(1-x)^2 + \tau R_0 \Delta a\,(1-x) \tag{24}$$

Note that the solution of (23) is obtained as

$$Z(x) = \frac{B}{k} - \frac{B'}{k^2} + \frac{B''}{k^3} + c\,\exp(-k\,x) \tag{25}$$

Since k is large for long-range engagements, the last term of the right-hand side(RHS) of (25) diminishes to zero quickly. Then, the solution of (25) is approximated as

$$Z(x) = R_0\,b_0(1-x)^2 + \frac{R_0}{k}(2\,b_0 + \tau\,\Delta a)(1-x) + \frac{R_0}{k^2}(2\,b_0 + \tau\,\Delta a) \tag{26}$$

The first two terms of the RHS of (26) goes to zero at the terminal time since the normalized downrange x goes to 1 as the missile approaches to the PIP. Therefore, the last term becomes the miss distance of the APG defined by (18), which is rewritten as

$$\text{Miss Distance} = \frac{V_m^2 R_0}{N^2 X_f^2}\left(2 b_0 + \frac{X_f}{V_m^2}\Delta a\right) = \frac{2 V_m^2 R_0}{N^2 X_f^2} b_0 + \frac{R_0}{N^2 X_f}\Delta a \tag{27}$$

Using the approximation that $R_0 \approx X_f$, we can further simplify the expression of the miss distance as

$$\text{Miss Distance} = \frac{1}{N^2}\left(\frac{2 V_m b_0}{t_f} + \Delta a\right) \tag{28}$$

<u>Lead-Angle Tracking Error</u>

Equation (26) can be rewritten as

$$R\,\lambda = R\,\lambda_{com} + \frac{RV_m}{NX_f}(2\,b_0 + \tau\,\Delta a) + \frac{V_m^2}{N^2 X_f}(2\,b_0 + \tau\,\Delta a) \tag{29}$$

or

$$\lambda - \lambda_{com} = \frac{V_m}{NX_f}\left[1 + \frac{V_m}{NR}\right](2\,b_0 + \tau\,\Delta a) \tag{30}$$

which shows that the error of λ in tracking λ_{com} remains almost constant until R is reduced to a small value. When $R = V_m / N$, the second term in the bracket of (30) becomes equal to the first term. This implies that the divergence of the tracking error of λ becomes significant only when the time to go is reduced to the order of $1/N$.

DOI: 10.13009/EUCASS2023-519

4. Numerical Experiments

One of the merits of the proposed trajectory shaping method is that it is independent of the missile's dynamic charateristics. However, the reference trajectory may not be achieved if the required acceleration is not generated. This problem can happen if the peak altitude of the reference trajectory is very high. Several numerical experiments are conducted to investigate this issue and to confirm the analysis results obtained in the previous section. A typical long-range air-to-air missile model used in [2] is employed here for trajectory simulation. The equations of motion of the missile in the vetical plane is as follows :

$$\dot{X} = V \cos\gamma \tag{7}$$

$$\dot{Z} = -V \sin\gamma \tag{8}$$

$$\dot{V} = \frac{T\cos\alpha - D}{m} - g\sin\gamma \tag{9}$$

$$\dot{\gamma} = \frac{T\sin\alpha + L}{m\,V} - \frac{g\sin\gamma}{V} \tag{10}$$

$$\dot{m} = -\frac{T}{I_{sp}\,g} \tag{11}$$

where the Z-axis is positive downward, m is the mass, T is the thrust, I_{sp} is the specific impulse, L is the lift, D is the drag, g is the gravitational acceleration, and α is the angle of attack. The missile is launched from a fighter flying at 10 km altitude with a speed of 300 m/s. It has two solid-propellant rockets ignited sequentially without a coasting phase between them. The target of the midcourse guidance phase is a PIP located at a downrange of 100 km with 5 km altitude. In this simulation, the angle of attack is calculated from the acceleration command but it is limited within 20 degrees. A linear lift model of $C_{L\alpha}$ =10 is employed, which is acceptable when the angle of attck is limited. The autopilot lag is ignored since the time constant of the autopliot dynamics is very short when compared with the total flight time. A realistic drag model including the additional drag induced by the lift is employed. Finally, the guidance gain of APG is chosen as $N = 2$.

Figure 4 shows the simulation results of the quadratic trajectory treated in Example 1. In this simulation, λ_0 is chosen as 58.3 deg, which maximizes the terminal speed for $C_{L\alpha}$ =10. It is observed that the trajectory shape is dependent to the lift derivative $C_{L\alpha}$. Since the maneuver capability of the vehicle is significantly limited at high altitudes around 30 km, the lead angle can not be controlled well for this reference trajectory. As shown in Figure 5, the lead-angle tracking error is reduced if the missile is designed to have higher $C_{L\alpha}$'s.

It is interesting to obseve that the terminal speed with $C_{L\alpha}$ =10 is higer than that with $C_{L\alpha}$ =12.5 or 15. The trajectory simulations give the terminal speed as 869.9 m/s, 825.8 m/s, and 804.9 m/s for $C_{L\alpha}$ of 10, 12.5 and 15, respectively. This result is not surprising since a higher trajectory produces a higher terminal speed. The miss distances are found to be 2.5 m, 2.0 m, and 1.7 m for $C_{L\alpha}$ of 10, 12.5 and 15, respectively. For this engagement scenario, the values of V_m, t_f, and b_0 are approximately 1,000 m/s, 100 sec, and 1 rad, respectively. Hence, the first term of (28) is estimated as 5 m, which complies with the simulation results.

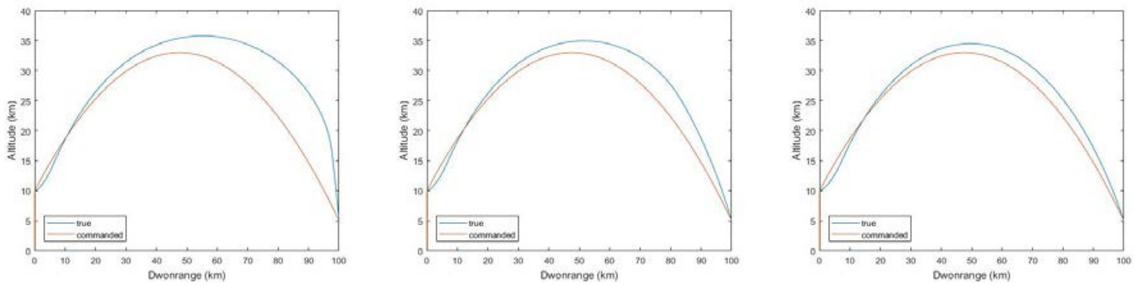

(a) $C_{L\alpha} = 10$ (b) $C_{L\alpha} = 12.5$ (c) $C_{L\alpha} = 15$

Figure 4: Quadratic Trajectories for Various Lift Coefficients

DOI: 10.13009/EUCASS2023-519

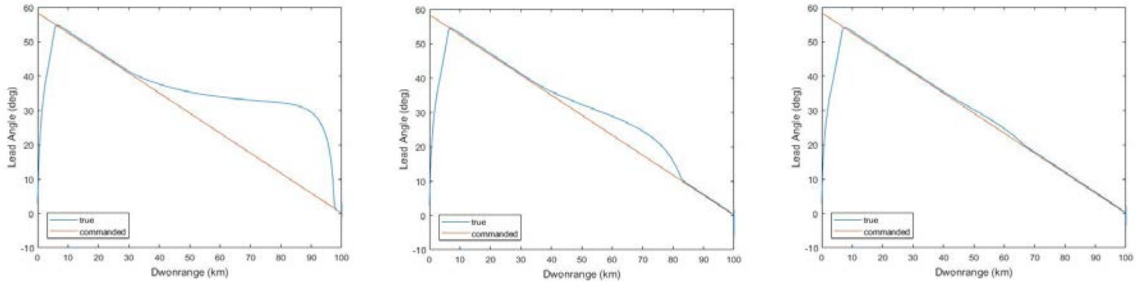

(a) $C_{L\alpha} = 10$ (b) $C_{L\alpha} = 12.5$ (c) $C_{L\alpha} = 15$

Figure 5: Lead Angle Histories for Various Lift Coefficients

For the fourth-order trajectory treated in Example 3, the simulated trajectory is insensitive to $C_{L\alpha}$ and the lead-angle tracking error is less than 1 deg, as shown in Figure 6. When the flight altitude is limited to 20 km, the missile is capable of controlling the lead angle even for the case of $C_{L\alpha}$ = 10. However, the terminal speed is significantly reduced to 572.2 m/s for the fourth-order trajectory due to the darg increase at low altitudes.

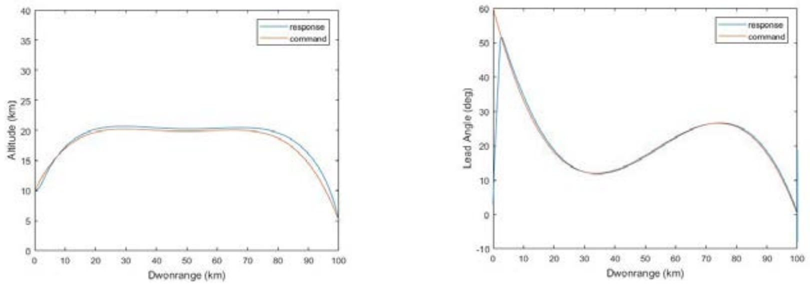

(a) Trajectory (b) Lead Angle

Figure 6: Simulation Results of the Fourth-order Trajectory

One of the motivation of this study is that the optimal trajectory maximizing the terminal speed is very close to a quadratic trajectory. Since the quadratic trajectory has a single parameter λ_0 to choose, a suboptimal trajectory for terminal speed maximation can be easily determined by a linear search over a suitable region of λ_0. Table 1 [2] compares the terminal speed of the optimal trajectory calculated by GPOPS-II, a commercial trajectory optimization software, with that of the suboptimal trajectory for various PIP altitudes. Table 1 also provides the filght time and the optimal value of λ_0 found for each suboptimal trajectory. It is observed that the difference in terminal speed is less than 2.8 % for all PIP altitudes. An extensive study on the APG based on linear lead-angle command for midcourse guidance of the same missile model can be found in Ref. [2].

5. Conclusions

This work has proposed a new trajectory shaping method for midcourse guidance of long-range air-to-air missiles. The key idea is to generate polynomial-type trajectories by introducing polynomial type lead-angle biases to the conventional pursuit guidance law. To provide a theoretical foundation, we have demonstrated that the lead-angle bias is equivalent to the lead-angle command and APG is able to control the lead angle to track the lead angle command faithfully if the missile has sufficient maneuver capability. Furthermore, the miss-distance characteristics are investigated to show that APG is able to hit stationary targets with a meter-level accuracy. Although the analytical investigation has been conducted only for the case of linear lead-angle command, the simulation results show that APG with a third-order lead-angle command, which generates a fourth-order trajectory, shares the same characteristics. The proposed method can be applied to various optimal guidance problems for which the optimal trajectory is well

DOI: 10.13009/EUCASS2023-519

approximated by a polynomial. For this type of problems, the suboptimal trajectoy is parameterized by using a few parameters that can be easily determined on line for real-time applications. The suboptimal trajectory can be used for the initiation of more sophisticated real-time trajectory optimization. APG has also a potential to be a real-time guidance method for various applications that prefer a simple and inexpensive midcourse guidance law to complex and computationally-intensive algorithms.

Table 1: Terminal Speed Optimization Results [2]

PIP (km)	Method	Flight Time (s)	Terminal Speed (m/s)	λ_0^* (deg)
[100, 20]	GPOPS	94.19	1182.27	
	APG	93.50	1170.98 (-1.0%)	43.2
[100, 15]	GPOPS	96.63	1147.52	
	APG	96.25	1135.91 (-1.0%)	48.4
[100, 10]	GPOPS	100.51	1061.62	
	APG	100.58	1046.86 (-1.4%)	53.5
[100, 5]	GPOPS	105.70	888.28	
	APG	106.38	869.90 (-2.1%)	58.3
[100, 0.1]	GPOPS	112.39	588.74	
	APG	114.12	572.48 (-2.8%)	62.7

Acknowledgements

This work was supported by the Theater Defense Research Center funded by the Defense Acquisition Program Administration under Grant UD200043CD. The authors are very thankful for the technical comments of the project monitors of Agency for Defense Development.

References

[1] Pastrick, H. L., Seltzer, S. M., and Warren, M. E. 1981. Guidance laws for short-range tactical missiles. *Journal of Guidance and Control.* 4(2): 98-108.

[2] Tahk, M. J., Park, J. C., Roh, H., and Lee, C. H. 2023. Suboptimal guidance based on pursuit and impact angle control for long-range air-to-air missiles. In: *14th International Conference on Mechanical and Aerospace Engineering (ICMAE)*, Porto, Portugal.